J Electr Eng Technol Vol. 7, No. 6: 859-868, 2012
http://dx.doi.org/10.5370/JEET.2012.7.6.859

ISSN(Print) 1975-0102
ISSN(Online) 2093-7423

Development of Fault Location Algorithm and Its Verification Experiments for HVDC Submarine Cables

Chae-Kyun Jung*, Hung-Sok Park*, Ji-Won Kang*, Xinheng Wang, Yong-Kab Kim*** and Jong-Beom Lee†**

Abstract – A new fault location algorithm based on stationary wavelet transform and its verification experiment results are described for HVDC submarine cables in this paper. For wavelet based fault location algorithm, firstly, 4th level approximation coefficients decomposed by wavelet transform function are superimposed by correlation, then the distance to the fault point is calculated by time delay between the first incident signal and the second reflected signal. For the verification of this algorithm, the real experiments based on various fault conditions and return types of fault current are performed at HVDC submarine cable test yard located in KEPCO(Korea Electric Power Corporation) Power Testing Center of South Korea. It proves that the fault location method proposed in this paper is very simple but very quick and accurate for HVDC submarine cable fault location.

Keywords: Approximation coefficient, HVDC submarine cables, Fault location, Wavelet transform

1. Introduction

HVDC submarine cable is usually used to connect the power system between long distance islands. If the fault occurs on this submarine cable, it is very difficult to detect the fault point because it is installed under the deep sea as well as the cable is very long [1]. For instance, the total length of a HVDC submarine cable that provides services in South Korea is approximately over l00 km and the depth of sea water is over 100m [2]. Also, the delay of accurately detecting the fault location may incur excessive economical damage because of extended recovery time. Generally, one of the most useful methods for fault location of submarine cable is TDR(Time domain reflectrometer). However, it is very difficult to understand the measured TDR waveforms. In addition it is very complicated to operate. So, extensive experience and special training are required for operators [3, 4].

Generally, wavelet transform is very useful in signal processing and filter design for fault location because it has the ability to localize the signals in both time and frequency domains. The benefits of applying wavelet transform in fault location of power system have already been recognized by many researchers [5-12]. However, the wavelet transform itself has limitations for accurate fault location because there are many irregular waveforms in measured original signal. Therefore, in this paper, a new fault location algorithm based on stationary wavelet transform is proposed for fault location of HVDC submarine cable. Firstly, the signal is measured by oscilloscope after injecting a pulse on faulty phase. The measured signal is decomposed by 4^{th} level wavelet transform. Then each level approximation is superimposed by correlation. Many noises can be removed from this process. Finally, the distance to the fault point can be calculated by time delay between the first incident signal and the second reflected signal. The proposed algorithm is also verified by the real experiments according to various fault conditions and return types of fault current at HVDC submarine cable test yard located in KEPCO Power Testing Center in Korea. From these results, the effectiveness of new fault location algorithm for submarine cable is sufficiently proved.

After brief review of the structure and parameters of HVDC submarine cable in second section, the stationary wavelet transform and wavelet based new fault location algorithm will be described in Sections 3 and 4. The algorithm will be tested by real experiments in Section 5. The last section concludes the paper.

2. Structure and Parameters of HVDC Submarine Cables

The type of HVDC submarine cable used for experiments of new fault location algorithm is 800 mm^2 CUMI, which is a cable on real HVDC system between Jeju and Haenam that is presently operating in South Korea. Fig. 1 and Table 1 show the structure and the mechanical and electrical parameters of this cable, respectively.

† Corresponding Author : Dept. of Electrical Engineering, Wonkwang University, Korea. (ipower@wonkwang.ac.kr)
* Power System Laboratory, KEPCO Research Institute, Korea. (chekyun@kepri.re.kr, parkhs@kepco.co.kr, jwkang@kepri.re.kr)
** School of Engineering, Swansea University, United Kingdom(UK). (xinheng.wang@swansea.ac.uk)
*** Dept. of Information Communication Engineering, Wonkwang University, Korea (ykim@wonkwang.ac.kr)
Received: April 12, 2011; Accepted July 16, 2012

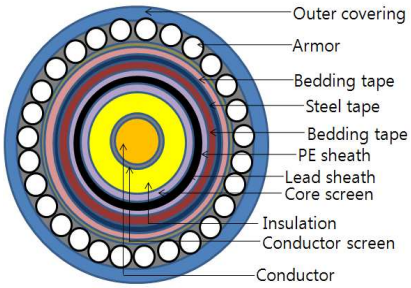

Fig. 1. Structure of CUMI 800 mm^2 cable

Table 1. Mechanical and electrical parameters of 800 mm^2 CUMI cable

	Thickness (t[mm])	Diameter (D[mm])	Remarks
Conductor	-	32.6	Resistivity = 1.724 μΩ·cm
Conductor Screen	0.6	33.8	-
Insulation(MI paper)	9.5	52.8	Permittivity = 4.3
Core Screen	0.45	53.6	-
Lead Sheath	2.7	59.1	Resistivity = 20.4 μΩ·cm
PE Sheath	3.2	65.5	Permittivity = 2.3
Bedding Tape	0.35	66.2	-
Reinforcement (Steel Tape)	2×0.3	67.4	-
Bedding Tape(PP)	1.2	69.8	-
Armor (Galvanized Steel, 37Wire Φ6)	6.15	82.1	Resistivity = 10 μΩ·cm
Outer Covering	4.1	90.3	Permittivity = 2.2

3. Stationary Wavelet Transform

In this section, the basic principle of the stationary wavelet transform will be presented. Stationary wavelet transform uses upsampling at each level of decomposition that causes redundancy. In wavelet transform, the number of elements per scale and location are fixed independent of scale. The redundancy increases the elements per scale and location at coarse scales. In term of denoising, there is an advantage of having more orientations than necessary at coarse scales. Because of this characteristic, stationary wavelet transform is better applied in noise signal processing [13, 14].

The stationary wavelet transform can be described as at each level, when the high and low pass filters are applied to the data, the two new sequences have the same length as the original sequences. To do this, the original data is not decimated. However, the filters at each level are modified by padding them out with zeros.

Supposing a function $f(x)$ is projected at each step j on the subset V_j ($\ldots\ldots \subset V_3 \subset V_2 \subset V_1 \subset V_0$), this projection is defined by the scalar product $c_{j,k}$ of $f(x)$ with the scaling function $\varphi(x)$ which is dilated and translated as in Eqs. (1) and (2):

$$c_{j,k} =< f(x), \varphi_{j,k}(x) > \tag{1}$$

$$\varphi_{j,k}(x) = 2^{-j}\varphi(2^{-j}x - k) \tag{2}$$

where $\varphi(x)$ is the scaling function, which is a low-pass filter, $c_{j,k}$ is also called a discrete approximation at the resolution 2^j, j is the scale and k is the translation.

If $\phi(x)$ is the wavelet function, the wavelet coefficients are obtained by:

$$\omega_{j,k} =< f(x), \quad 2^{-j}\phi(2^{-j}x - k) > \tag{3}$$

where $\omega_{j,k}$ is called the discrete detail signal at the resolution 2^j.

As the scaling function $\phi(x)$ has the property: $\frac{1}{2}\varphi(\frac{x}{2}) = \sum_n h(n)\varphi(x-n)$, where $h(n)$ is the low-pass filter, $c_{j+1,k}$ can be obtained by direct computation from $c_{j,k}$

$$c_{j+1,k} = \sum_n h(n-2k)c_{j,n} \text{ and } \frac{1}{2}\varphi(\frac{x}{2}) = \sum_n g(n)\phi(x-n) \tag{4}$$

where $g(n)$ is the high-pass filer.

The scalar products $< f(x), 2^{-(j+1)}\phi(2^{-(j+1)}x - k) >$ are computed with:

$$\omega_{j+1,k} = \sum_n g(n-2k)c_{j,n} \tag{5}$$

Eqs. (4) and (5) are the multi-resolution algorithms of the traditional discrete wavelet transform. In this transform, a downsampling algorithm is used to perform the transformation. That is one point out of two is kept during transformation. Therefore, the whole length of the function $f(x)$ will be reduced by half after the transformation. This process continues until the length of the function becomes one.

However, for stationary or redundant transform, instead of downsampling, an upsampling procedure is carried out before performing filter convolution at each scale. The distance between samples increases by a factor of 2 from scale j to the next. $c_{j+1,k}$ is obtained by:

$$c_{j+1,k} = \sum_l h(l)c_{j,k+2^j l} \tag{6}$$

and the discrete wavelet coefficients are:

$$\omega_{j+1,k} = \sum_{l} g(l) c_{j,k+2^j l} \tag{7}$$

where l indicates the finite length.

4. Wavelet Based Fault Location Algorithm

The transient signal decomposed by wavelet transform shows clearly high value at the fault point, while the magnitudes of the other transients are relatively low. It is discovered that the wavelet maxima at a scale 2^j will propagate to another maxima at the coarser scale 2^{j+1}. The number of maxima is also reduced by increasing of scale. Through this wavelet transform characteristics, the correlation of approximation of wavelet transform can detect the reflection points of travelling wave.

For the white noises, on average, the number of maxima decreases by a factor of 2 when the scale increases by 2. Half of the maxima do not propagate from the scale 2^j to the scale 2^{j+1}. We adopted a simple algorithm to remove the noise relied on the variations in the scale of the wavelet transform data of the signal by using direct multiplication of the wavelet data at adjacent scales [15].

Generally, underground power cable systems including submarine cable use the detail signal with high frequency component for fault location when the fault occurs on the system because the fault signals include high frequency components. However, in this paper, the approximation coefficient of low frequency component is used for fault location of HVDC submarine cable. The approximation has an advantage for fault location analysis using injection of pulse because high frequency component is less in measured signals.

The original signal can be captured by oscilloscope after surge pulse which is the same as TDR being injected to faulty phase. Then the measured signal is decomposed by stationary wavelet transform. Finally, it is superimposed by correlation of multiple steps approximation coefficients. Many noises between the first incident signal and the second reflection are removed from this process.

Fig. 2 shows the whole procedure of fault location algorithm for HVDC submarine cables. As shown in this procedure, firstly, the signal will be measured by oscilloscope after injecting a pulse on faulty phase. The measured signal will be decomposed by stationary wavelet transform. Where, supposing the signal is decomposed by wavelet at *n* levels, the approximation coefficients will be A_1, A_2, …, A_n. Then approximations at first four scales will be multiplied directly as shown in Eq. (8), give a correlation 'Corr'. Finally, the distance to fault point can be calculated by time difference and propagation velocity.

$$Corr = A_1 \times A_2 \times A_3 \times A_4 \tag{8}$$

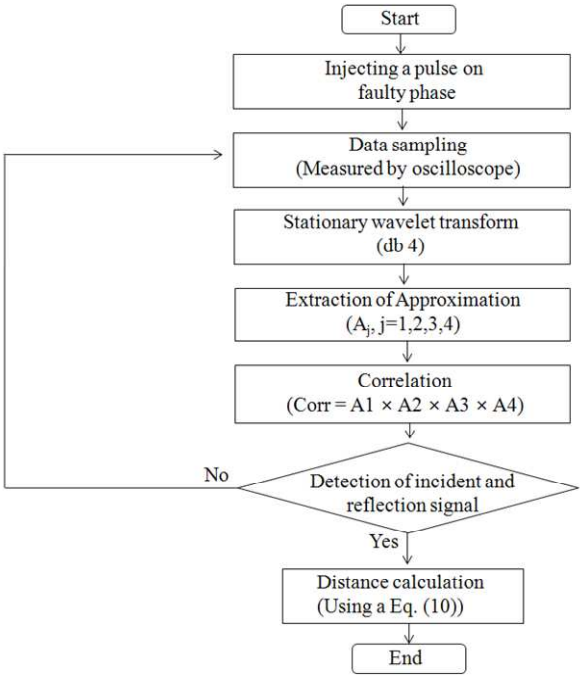

Fig. 2. Flow chart for fault location algorithm

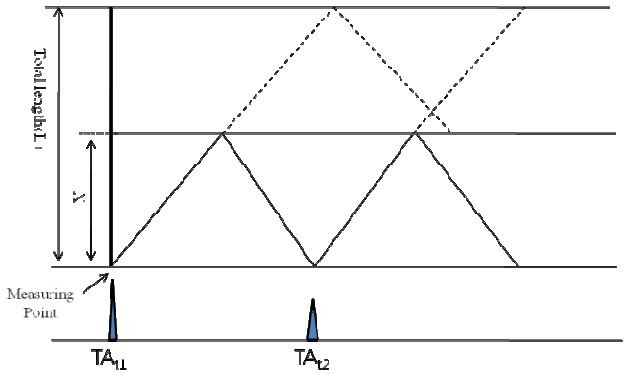

Fig. 3. Lattice diagram

Fig. 3 shows the lattice diagram of the characteristic of travelling wave as the fault occurs on the test HVDC submarine cable. In this case, the arrival time of the first incident signal (TA_{t1}) and second reflection(TA_{t2}) at measuring point are detected using correlation of approximations. The distance(X) to the fault point can be calculated by Eq. (9). This approach to locate the fault is simple and quick, but very accurate. The wavelet function applied in this algorithm is 'db4'.

$$X = \frac{\upsilon \cdot (TA_{t2} - TA_{t1})}{2} \tag{9}$$

where υ is the propagation velocity on HVDC submarine cable and TA_{t1} and TA_{t2} are the arrival times of first incident and second reflected signal, respectively.

5. Verification Experiments

The actual tests of 7 test conditions are performed in this paper according to grounding fault conditions in two test HVDC submarine cables with total length of 194 m and 80 m, respectively. Figs. 4 and 5 show the system diagram of two test cables. As shown in these figures, the test cable 1 of 194m has fault point at 48 m from measuring point, but there is no fault on the test cable 2 of 80 m. Also, the termination of both test cables is open. The artificial ground fault is considered by electrode between core and sheath. The propagation velocity of test cable is 142.4 m/㎲. This is proved by the TDR test.

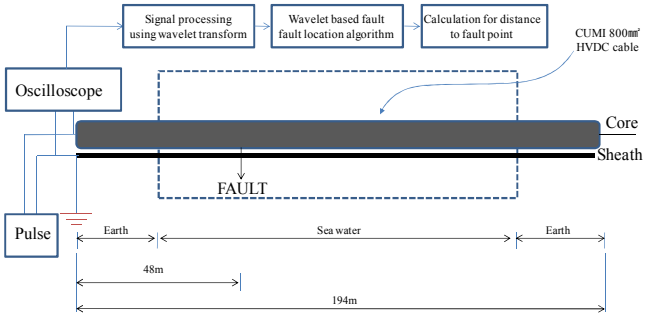

Fig. 4. Test HVDC submarine cable 1 (total length : 194 m, fault point : 48 m)

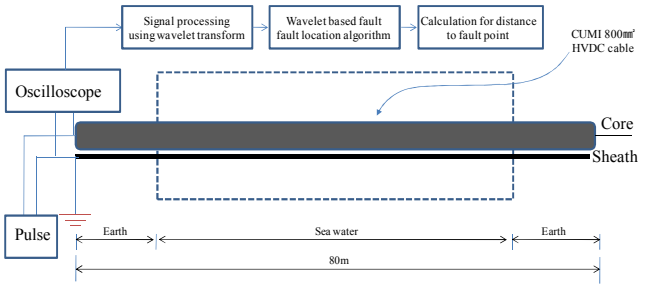

Fig. 5. Test HVDC submarine cable 2 (total length : 80 m)

Table 2 shows the real test conditions. As shown in Table 2, Test cable 1 is used for Test 1 to Test 6. Test 7 is performed on Test cable 2. The propagation velocity of all test conditions is 142.4 m/㎲. In Test 1, the electrode between the core and sheath is solidly connected for artificial ground fault at 48 m from measuring point, and fault current is returned through earth. In Tests 2 and 3, the fault condition is equal to Test 1, but Delta T and return path of fault current are just changed to 4.0E-9 s and sea water, respectively. In Test 4, the electrode gap is increased from Test 3 in order to increase the fault resistance. In Test 5, the return path of fault current is changed to earth. Test 6 increases the electrode gap to increase the fault resistance for the returned fault current by earth. Test cable 2 is used for Test 7.

The unit of X-axis is changed by sampling point after wavelet transform of waveforms measured by oscilloscope. Therefore, the distance to fault point of Eq. (9) can be converted by application of sampling point and delta T(Δt) as shown in Eq. (10).

Table 2. Real test conditions

Test	Test conditions
Test 1	· Test HVDC submarine cable 1 , velocity(υ) : 142.4 m/㎲ · Delta T(Δt) : 2.0E-9 s · Fault current is returned through earth · Fault condition : solid connection of electrode between core and sheath
Test 2	· Test HVDC submarine cable 1 , velocity(υ) : 142.4 m/㎲ · Delta T(Δt) : 4.0E-9 s · Fault current is returned through earth · Fault condition : solid connection of electrode between core and sheath
Test 3	· Test HVDC submarine cable 1 , velocity(υ) : 142.4 m/㎲ · Delta T(Δt) : 2.0E-9 s · Fault current is returned through sea water(using 15 ground rods) · Fault condition : solid connection of electrode between core and sheath
Test 4	· Test HVDC submarine cable 1 , velocity(υ) : 142.4 m/㎲ · Delta T(Δt) : 2.0E-9 s · Fault current is returned through sea water(using 15 ground rods) · Fault condition : increasing an electrode gap distance between core and sheath
Test 5	· Test HVDC submarine cable 1 , velocity(υ) : 142.4 m/㎲ · Delta T(Δt) : 2.0E-9 s · Fault current is returned through earth(using 15 ground rods) · Fault condition : solid connection of electrode between core and sheath
Test 6	· Test HVDC submarine cable 1 , velocity(υ) : 142.4 m/㎲ · Delta T(Δt) : 2.0E-9 s · Fault current is returned through earth(using 15 ground rods) · Fault condition : increasing an electrode gap distance between core and sheath
Test 7	· Test HVDC submarine cable 2 , velocity(υ) : 142.4 m/㎲ · Delta T(Δt) : 4.0E-9 s

$$X = \frac{\upsilon \cdot (TA_{p2} - TA_{p1}) \cdot \Delta t}{2} \tag{10}$$

where υ is propagation velocity on HVDC submarine cable, TA_{p1} and TA_{p2} are the sampling point of the first incident and the second reflected signal, respectively, and Δt is decided by the sampling rate of oscilloscope.

The criterion used for evaluating the algorithm is the location error which is defined as

$$\text{Error}(\%) = \frac{|\text{actual location-calculated location}|}{\text{total line length}} \times 100 \tag{11}$$

Fig. 6 shows the measured original waveform of Test 1. The fault point of Test 1 is 48m from measuring point, fault current is returned through earth. As shown in Fig. 6, it is

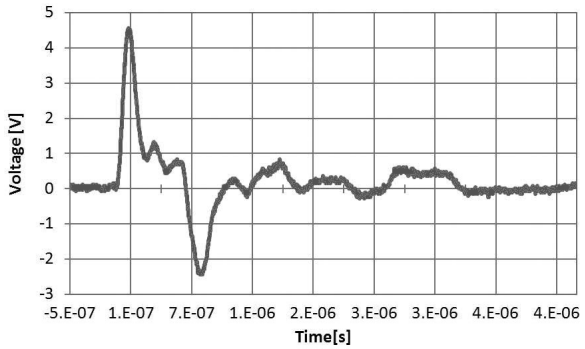

Fig. 6. Original waveform measured by oscilloscope (Test 1)

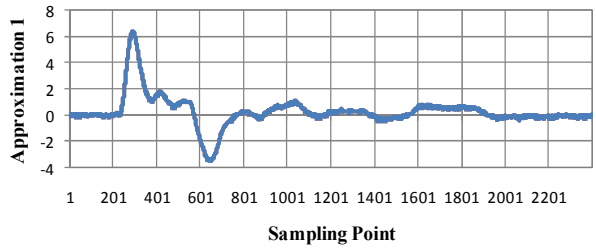

(a) Approximation 1(A1)

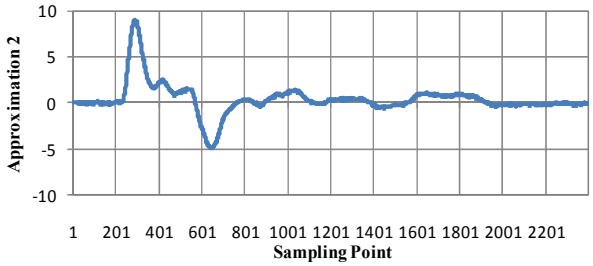

(b) Approximation 2(A2)

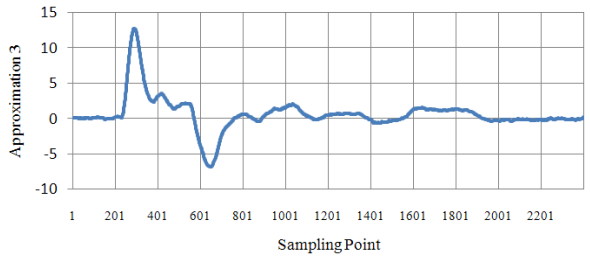

(c) Approximation 3(A3)

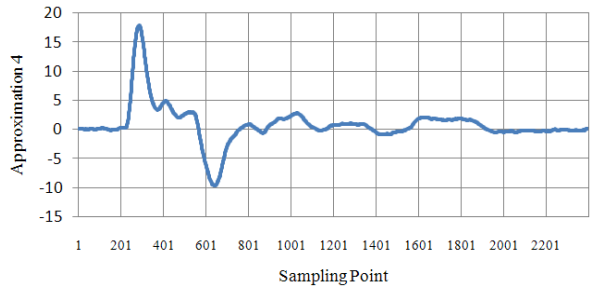

(d) Approximation 4(A4)

Fig. 7. Each approximation result of 4 levels wavelet transform (Test 1)

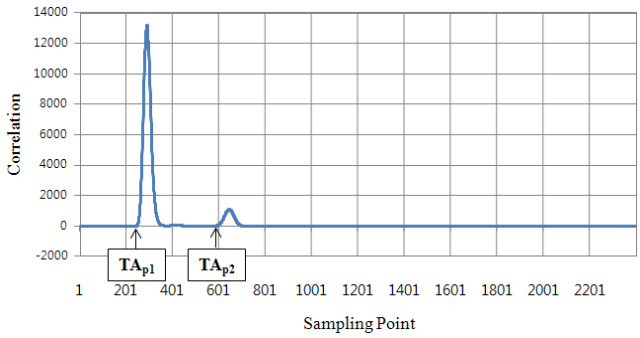

Fig. 8. Multiple scales correlation of approximations (Test 1)

difficult to discriminate the second reflected signal because of the various waveform types and noises. Fig. 7 shows each approximation result of 4 levels stationary wavelet transform. Finally the second reflection point can be obviously discriminated after rescaling using multiple scales correlation of approximations as shown in Fig. 8. Therefore, the distance to the fault point can be calculated. In this case, Δt is 2E-9 s, the sampling points of the first(incident) and the second(reflection) are 242 and 580, and propagation velocity is 1.424×105 km/s. The calculated distance is 48.13 m as shown in Eq. (12) which is very close to the exact fault distance of 48 m. The error rate is just 0.06 %.

$$X = \frac{(1.424\times10^{5})\cdot(580-242)\cdot(2E-9)}{2}\times1000 = 48.13[m] \tag{12}$$

$$Error(\%) = \frac{|48-48.13|}{194}\times100 = 0.06[\%] \tag{13}$$

In case of Test 2, the test condition is the same as Test 1, but sampling rate is changed on oscilloscope. Fig. 9 shows the measured original waveform of Test 2. Fig. 10 shows the rescaling waveform using multiple scales correlation of approximations. As shown in Fig. 10, the second reflection point can be obviously discriminated for fault location. Δ t of Test 2 is 4E-9 s. It is twice of Test 1. The sampling points

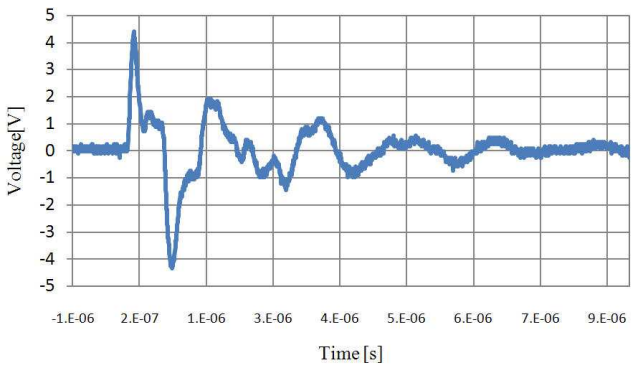

Fig. 9. Original waveform measured by oscilloscope (Test 2)

of the first and the second arrival times are 271 and 440, and the calculated distance is 48.1 m as shown in Eq. (14) which is also very close to the exact fault distance of 48 m. The error rate is just 0.05 %. It is more accurate than Test 1. The accuracy of fault location can be increasing.

$$X = \frac{(1.424\times10^5)\cdot(440-271)\cdot(4E-9)}{2}\times1000 = 48.10[m] \tag{14}$$

$$Error(\%) = \frac{|48-48.1|}{194}\times100 = 0.05[\%] \tag{15}$$

Fig. 11 shows the system diagram of Test 3. As shown in Fig. 11, the grounding type is changed by sea water return type. 15 ground rods are also installed for maximizing the grounding effects. The total length and fault point of test cable is the same as in Test 1 and Test 2.

Fig. 12 shows the original signal captured by oscilloscope, and Fig. 13 is each approximation result of 4th level wavelet transform. As shown in these figures, the waveform becomes easy slope comparing with Tests 1 and 2. Therefore, it is more difficult to discriminate the second reflected signal. However, after rescaling using multiple scales correlation of approximations, the noise is significantly removed. As shown in Fig. 14, the reflected point can be easily detected. Finally, the distance to fault point can be calculated by the time difference. In this case, Δt is 2E-9 s, the calculated distance is 48.8 m which is also very close to the exact fault distance of 48 m. The error

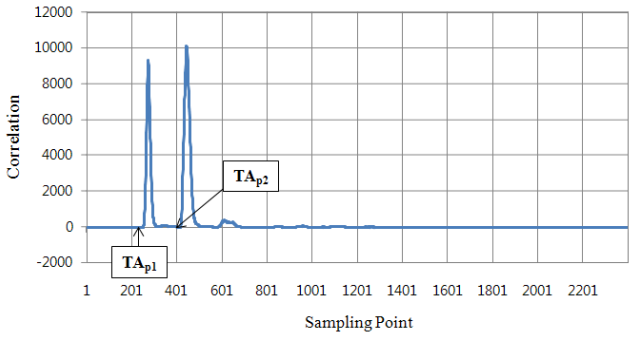

Fig. 10. Multiple scales correlation of approximations (Test 2)

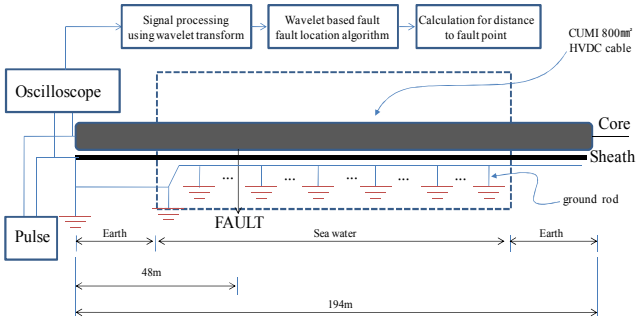

Fig. 11. System diagram of Test 3

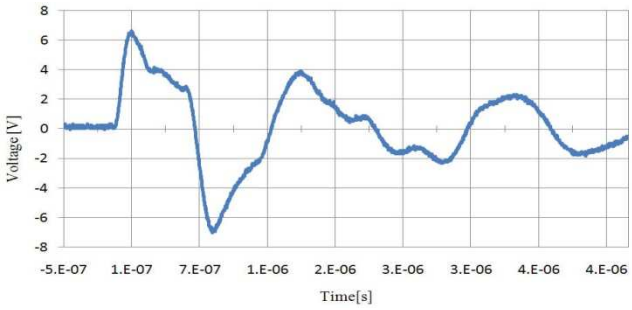

Fig. 12. Original waveform measured by oscilloscope (Test 3)

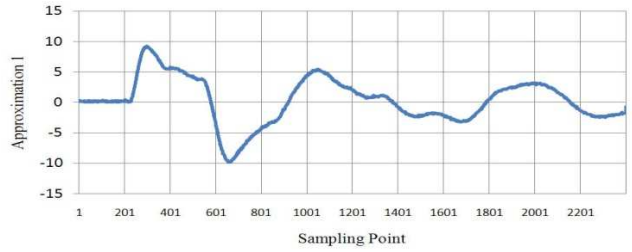

(a) Approximation 1(A1)

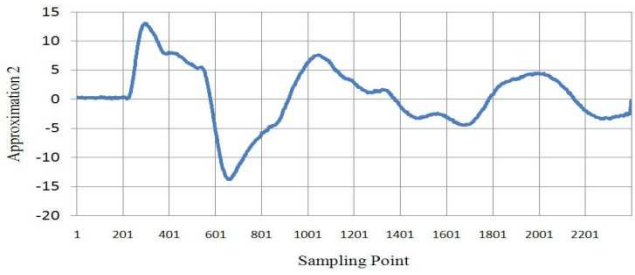

(b) Approximation 2(A2)

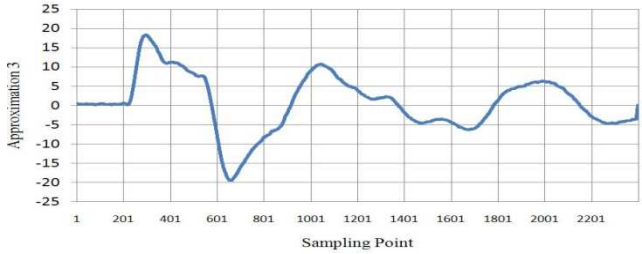

(c) Approximation 3(A3)

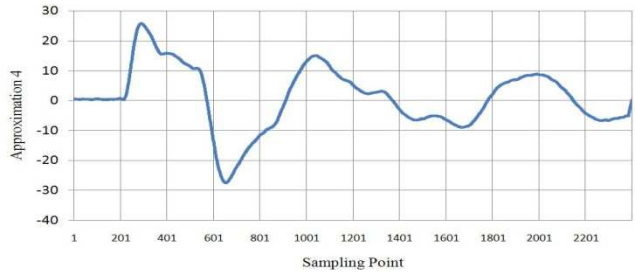

(d) Approximation 4(A4)

Fig. 13. Each approximation result of 4th level wavelet transform (Test 3)

rate is just 0.41 %.

In Test 4, the gap distance between core and sheath is expanded for increasing a fault resistance of fault point at fault condition of Test 3. Fig. 15 shows the captured original waveform by oscilloscope. As shown in figure, it is also hard to discriminate the exact second reflected point. However, the first and the second reflection point can be obviously discriminated for fault location through rescaling waveform using multiple scales correlation of approximations as shown in Fig. 16. In this case, the calculated distance is 47.9 m, and the error rate just shows 0.05 %. Therefore, it proves that the fault resistance has no big influence for fault location using new fault location algorithm proposed in this paper.

In Test 5, the return path of fault current is just changed by earth in sea water of Test 3. Fig. 17 is the original signal. Fig. 18 shows the signal after rescaling waveform using multiple scales correlation of approximations. As shown in Fig. 18, the first and the second reflection point can be obviously discriminated for fault location, the distance to fault point can be easily calculated. In this case, the calculated distance is 50.5 m, and the error rate shows 1.28 %. Although the calculation error is a little higher than other test conditions, it is still a low value.

In Test 6, the gap distance between core and sheath is expanded for increasing a fault resistance of fault point at fault condition of Test 5. Fig. 19 shows the captured original waveform by oscilloscope. Fig. 20 is the signal after rescaling waveform using multiple scales correlation of approximations. As shown in this figure, the first and the second reflection point can be obviously discriminated for fault location. The distance to fault point can be calculated as 50.5 m. It is equal to Test 5.

In Test 7, the sound HVDC submarine cable is used for fault location test as shown in Fig. 5. The total length is 80m, the core of opposite terminal is opened. The propagation velocity of Test 7 is the same as other tests, the

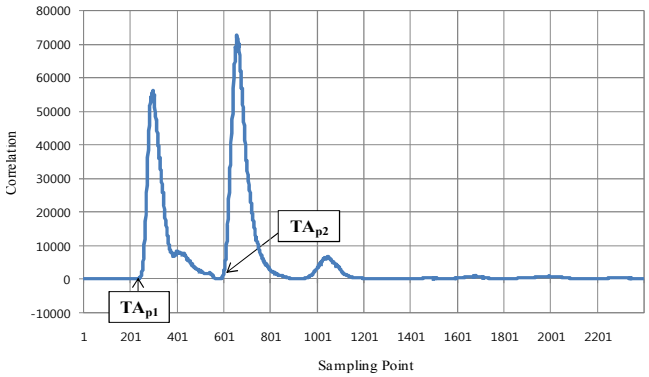

Fig. 14. Multiple scales correlation of approximations (Test 3)

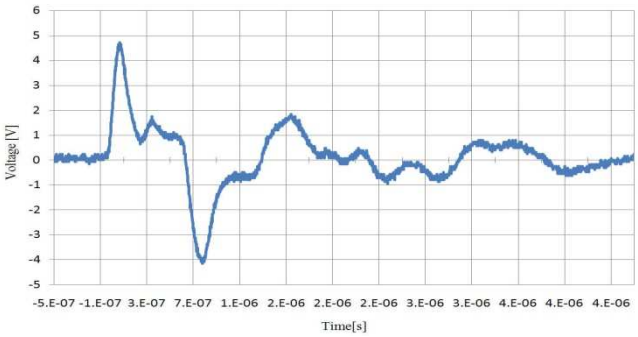

Fig. 15. Original waveform measured by oscilloscope (Test 4)

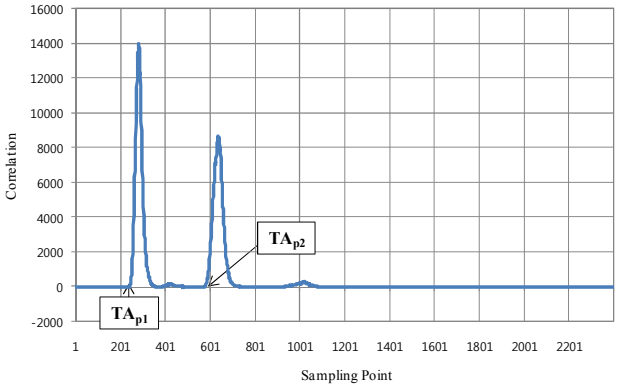

Fig. 16. Multiple scales correlation of approximations (Test 4)

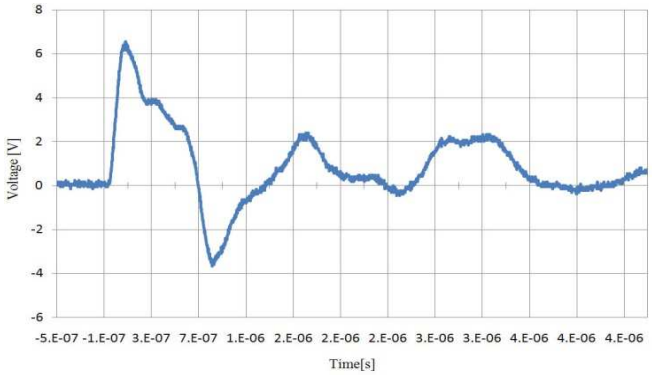

Fig. 17. Original waveform measured by oscilloscope (Test 5)

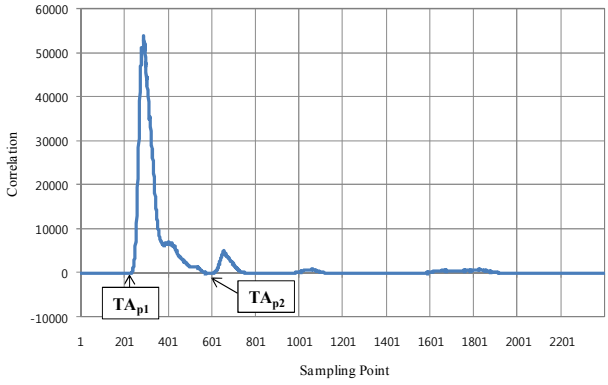

Fig. 18. Multiple scales correlation of approximations (Test 5)

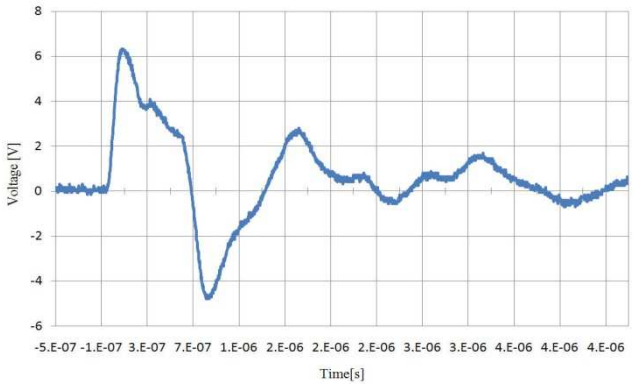

Fig. 19. Original waveform measured by oscilloscope (Test 6)

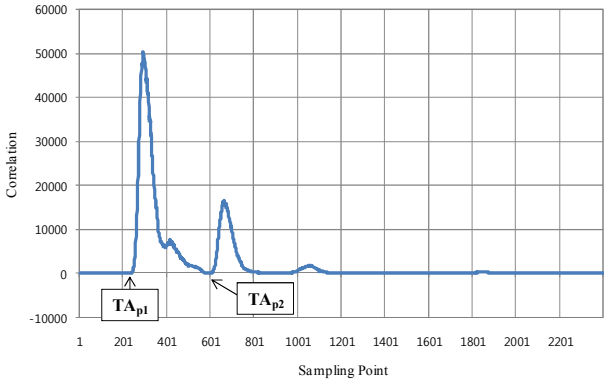

Fig. 20. Multiple scales correlation of approximations (Test 6)

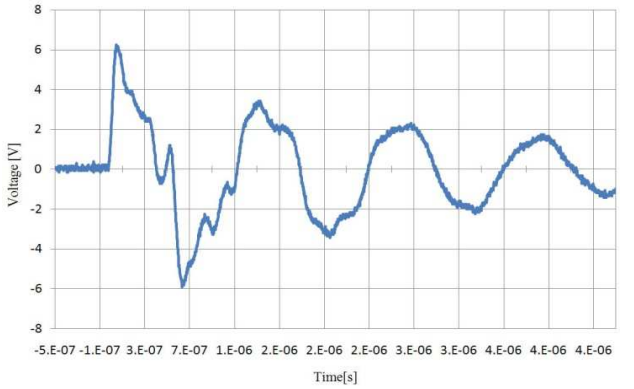

Fig. 21. Original waveform measured by oscilloscope (Test 7)

sampling rate is 4E-9 s. In this case, the location of opposite termination can be detected because there is no any fault point inside cable section.

Fig. 21 shows the captured original waveform by oscilloscope. Fig. 22 is the signal after rescaling waveform using multiple scales correlation of approximations. As shown in this figure, the first and the second reflection point can be obviously discriminated for opposite termination. From this result, the distance can be easily calculated. In this case, the sampling points of the first and

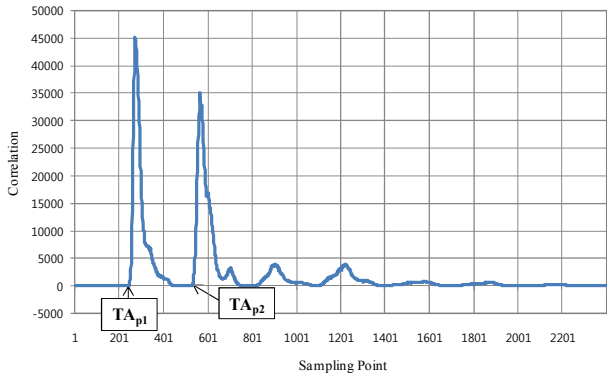

Fig. 22. Multiple scales correlation of approximations (Test 7)

Table 3. Calculation results of fault location for HVDC test submarine cable

Test	TA_{p2} [s]	TA_{p1} [s]	Actual distance [m]	Calculated distance [m]	Error [%]
Test 1	1.16e-6	4.84e-7	48	48.13	0.06
Test 2	1.76e-6	1.084e-6	48	48.1	0.05
Test 3	1.166e-6	4.8e-7	48	48.8	0.41
Test 4	1.156e-6	4.82e-7	48	47.9	0.05
Test 5	1.2e-6	4.9e-7	48	50.5	1.28
Test 6	1.18e-6	4.7e-7	48	50.5	1.28
Test 7	1.054e-6	4.86e-7	80	81.1	1.3
Average Error [%]					0.63

the second arrival times are 243 and 527, and propagation velocity is 1.424×10^5 km/s. The calculated distance and error rate are 81.1 m and 1.3 %, respectively.

The new fault location algorithm for HVDC submarine cable system has been tested for a variety of performed fault conditions. The maximum error rate is 1.3 % and the average error rate is 0.63 % that is less than 1 %. From these results, the accuracy of the new fault location algorithm proposed in this paper has been verified. The calculation results and error rate for fault location in all test conditions are shown in Table 3.

6. Conclusions

The new fault location algorithm based on stationary wavelet transform is proposed in this paper. The signals measured by oscilloscope are decomposed by wavelet transform. They are also rescaled by multiple scales correlation of approximations. In other words, the approximation coefficients at first four scales are multiplied directly in order to discriminate the incident and reflection point. Finally, the distance to fault point can be calculated by time delay between the first incident and the second reflection. The proposed algorithm is also verified by 7 test conditions performed at HVDC submarine cable test yard. The average error rate is 0.63%, and the results of all tests

show very accurate regardless of fault conditions. From these results, it is verified that the fault location algorithm proposed in this paper is very accurate and useful.

Acknowledgements

This work is the outcome of a Manpower Development Program for Marine Energy by the Ministry of Land, Transport and Maritime Affairs (MLTM)

References

[1] KEPCO, "Underground Transmission Cable System", Dec. 2002.

[2] J. S. Lee, B. S. Moon, W. T. Kang, K. S. Kim, "Introduction of Converter Station Construction for HVDC Link Project between Jindo and Jeju", 2009 *KIEE Summer Annual Meeting Proceedings*, July 2009.

[3] C. K. Jung, J. W. Park, K. H. Moon, B. M. Yang, J. W. Kang, "Validation of Propagation Velocity through TDR Test in HVDC Submarine Cables", *Transactions of KIEE*. Vol. 58, No. 10, Oct. 2009.

[4] C. K. Jung, B. M. Yang, J. K. Choi, K. H. Moon, J. W. Kang and J. B. Lee, "Simplified Fault Location Test Using Travelling Wave for HVDC Submarine Cables", *Proceeding of International Conference on Electrical Engineering*, July 2010.

[5] F.H. Magnago, A. Abur, "Fault location using wavelets" *IEEE Trans. On Power Delivery* Vol. 13, No. 4, pp. 1475-1480, 1998.

[6] E. Styvaktakis, M.H.J. Bollen, I.Y.H. Gu, "A fault location technique using high frequency fault clearing transients" *IEEE Power Eng. Rev.* Vol. 19, No. 5, pp. 50-60, 1999.

[7] M.M. Tawfik, M.M. Morcos, "A novel approach for fault location on transmission lines" *IEEE Power Eng. Rev.* Vol. 18, No. 11, pp. 58-60, 1998.

[8] A.M. Gaouda, S.H. Kanoun, M.M.A. Salama, A.Y. Chikhani. Generation, "wavelet-based signal processing for disturbance classification and measurement" *IEE Proc. Transmission & Distribution,* Vol. 149, No. 3, pp. 310-318, 2002.

[9] I.K. Yu, Y.H. Song, "Wavelet transform and neural network approach to developing adaptive single-pole auto-reclosing schemes for EHV transmission systems" *IEEE Power Eng. Rev.* Vol. 18, No. 11, pp. 62-64, 1998.

[10] F.N. Chowdhury, J.L. Aravenam "A modular methodology for fast fault detection and classification in power systems" *IEEE Trans. Control Syst. Technol.* Vol. 6, No. 5, pp. 623-634, 1998.

[11] Z.Q. Bo, M.A. Redfern, G.C. Weller, "Positional protection of transmission line using fault generated high frequency transient signal" *IEEE Trans. Power Deliv*, Vol. 15, No. 3, pp. 888-894, 2000.

[12] C.K. Jung, J.B. Lee, X.H. Wang, Y.H. Song, "Wavelet based noise cancellation technique for fault location on underground power cables", *Electric Power Systems Research(EPSR),* Vol. 77, issue 10, pp. 1349-1362, 2007.

[13] X.H. Wang, R.S.H. Istepanian, Y.H. Song, "Microarray image de-noising using stationary wavelet transform" *Proceeding of the 4th IEEE Conference Information Technology Applications*, pp. 15-18, 2003.

[14] H. Ye, G. Wang, S.X. Ding, "A new fault detection approach based on parity relation and stationary wavelet transform" *IEEE Proceeding of the American Control Conference,* pp. 2991-2996, 2003.

[15] Y. Xu, J. B. Weaver, D. M. Healy, J. Lu, "Wavelet transform domain filters : a spatially selective noise filtration technique", *IEEE Trans. Image Process*. Vol. 3, No. 6, pp. 747-758, 1994.

Chae-Kyun Jung received his B.Sc., M.Sc. and Ph.D. degrees in Electrical Engineering from Wonkwang University, Korea, in 1999, 2002 and 2006, respectively. He worked at University of Siegen as a post-doctor researcher from 2006 to 2007. He has been working at the KEPCO Research Institute from 2007 where he is currently a senior researcher in the Power System Laborotory. His research interests include power systems operation, analysis of power cable systems and fault location.

Hung-Sok Park received his B.Sc., M.Sc. and Ph.D. degrees in Electrical Engineering from Chungnam National Univeristy, Korea in 2003, 2005 and 2011, repectively. He has been working at the KEPCO Research Institute from 2008 where he is currently a researcher in the Power System Laborotory. His current research interests are power systems operation, analysis and diagnosis of power cable systems.

Ji-Won Kang received his B.Sc., M.Sc. and P.hD. degrees in Electrical Engineering from Hanyang University, Korea, in 1987, 1993 and 2003, respectively. He has been working at the KEPCO Research Institute from 1993 where he is currently a Principal researcher in the Power System Laborotory. His current research interests are power systems operation, analysis and diagnosis of power cable systems.

Xinheng Wang received his BEng and MSc degrees in electrical engineering from Xi'an Jiaotong University, China in 1991 and 1994, respectively, and his PhD degree in electronics and computing engineering from Brunel University, UK, in 2002. He is currently working as a senior lecturer in wireless communications in College of Engineering, Swansea University, UK, with research interests in systems condition monitoring, wireless networking, and wireless healthcare.

Yong-Kab Kim received his B.S degree in Electronics Engineering from Ajou University and the M.S.E degree in Electrical Engineering from University of Alabama in Huntsville. He received his Ph.D degree in Electrical & Computer Engineering in North Carolina State University. He is currently in Professor at Department of Information Communication Engineering, Wonkwang University, Korea. His research interests are Remote Sensing for Visible Communication, Optical Fiber Sensing, Power Line Communication.

Jong-Beom Lee received his B.Sc., M.Sc. and Ph.D. degrees in Electrical Engineering from Hanyang University, Korea, in 1981, 1983 and 1986, respectively. He worked at the Korea Electrotechnology Research Institute from 1987 to 1990. He was a Visiting Scholar at Texas A&M University and the Swiss Federal Institute of Technology (ETH), Switzerland. He is currently a Professor in the Department of Electrical Engineering, Wonkwang University, Korea. His current research interests are power systems operation, analysis of power cable systems and DC system.